Temperature Measurement of Carbon Nanotubes Using Infrared Thermography

Dorin Boldor,*,† Nicholas M. Gerbo,† William T. Monroe,† Jason H. Palmer,† Zhongrui Li,‡ and Alexandru S. Biris‡

Department of Biological and Agricultural Engineering, Louisiana State University Agricultural Center, 149 E. B. Doran Building, Louisiana State University, Baton Rouge, Louisiana 70803 and Nanotechnology Center, Applied Science Deptartment, University of Arkansas at Little Rock, Little Rock, Arkansas 72204

Received February 12, 2008. Revised Manuscript Received April 15, 2008

Multiwalled carbon nanotubes (MWNTs) have a very high absorbance in the near-infrared (NIR) region of the electromagnetic spectrum. It is demonstrated that the temperature of MWNTs, measured using infrared thermography during NIR laser irradiation, is much higher than that of other carbonaceous materials such as graphite controls. Since most biological materials have a low absorbance in the same region, carbon nanotubes could be used for selective photothermal hyperthermia of biological or nonbiological systems. This study was performed to prove the concept of direct measurement of the temperature distribution of carbon nanotubes when stimulated with laser irradiation. The maximum temperature increase of MWNTs measured with a high-sensitivity infrared camera, continuously irradiated with four 2.5-mW/650-nm lasers, was 7 °C vs a graphite control, while irradiation with a 390-mW/1064-nm laser yielded maximum temperature increases of more than 100 °C above the graphite control. The use of infrared thermography has allowed for specific data on laser-mediated heating kinetics of MWNTs to be presented here for the first time to our knowledge. These results could prove very useful in the design of selective photothermal processes of selectively destroying biological systems of interest.

1. Introduction

Carbon nanotubes (CNTs) are impressive structures that can be made in single- and multiwalled varieties of various lengths.[1] Their small size and unique electrical properties make them extremely attractive for a variety of applications in science and engineering fields. One potential application in life sciences that has attracted considerable interest is their use in cancer treatment. CNTs have a high absorbance in the near-infrared (NIR) spectrum, while biological tissues do not.[2–5] Specific optical absorbance data for CNTs has been reported in literature for a variety of tube diameters, chirality, and aggregation orientations and can vary depending on preparation methods and suspension solvents used.[6,7] Spectrophotometric data is difficult to acquire because CNTs are not water soluble, so most efforts to measure absorbance have included surface functionalization or use of an alternative solvent to dissolve the CNTs.[2,6–9] The thermal conductivity of CNTs, determined both empirically and numerically, over a wide range of values has been reported.[10–15] Individual CNTs have been shown to exhibit thermal conductivity as high as a few kW/mK in the axial dimension with values dropping below 100 W/mK for disordered porous films such as the ones used in the present study.[14,15] It is also noteworthy that adding CNTs to composite materials has been shown to significantly raise the thermal conductivity of the material.[16]

Hyperthermia treatment of cancer cells with nanoparticles (especially gold or other metals) has been demonstrated with some promising results in the past few years.[2,17] Gold nanoparticles have been investigated for their use in photo-

* To whom correspondence should be addressed. Phone: 225 578 7762. Fax: 225 578 3492. E-mail: dboldor@agcenter.lsu.edu.
† Louisiana State University.
‡ University of Arkansas at Little Rock.

(1) Loiseau, A. L. P.; Petit, P.; Roche, S.; Salvetat, J. *Understanding Carbon Nanotubes*; Springer: New York, 2006; p 667.
(2) Kam, N. W.; O'Connell, M.; Wisdom, J. A.; Dai, H. *Proc. Natl. Acad. Sci. U.S.A.* **2005**, *102*, 11600.
(3) Endo, M.; Iijima, S.; Dresselhaus, M. *Carbon Nanotubes*; Elsevier Science Limited: New York, 1996.
(4) Weissleder, R. *Nat. Biotechnol.* **2001**, *19*, 316.
(5) Delpy, D. T.; Cope, M. *Philos. Trans.: Biol. Sci.* **1997**, *352*, 649.
(6) Zhao, B.; Itkis, M. E.; Niyogi, S.; Hu, H.; Zhang, J.; Haddon, R. C. *J. Phys. Chem. B* **2004**, *108*, 8136.
(7) Zhao, B.; Itkis, M. E.; Niyogi, S.; Hu, H.; Perea, D. E.; Haddon, R. C. *J. Nanosci. Nanotechnol.* **2004**, *4*, 995.
(8) O'Connell, M. J.; Bachilo, S. M.; Huffman, C. B.; Moore, V. C.; Strano, M. S.; Haroz, E. H.; Rialon, K. L.; Boul, P. J.; Noon, W. H.; Kittrell, C.; Ma, J.; Hauge, R. H.; Weisman, R. B.; Smalley, R. E. *Science* **2002**, *297*, 593.
(9) Kataura, H.; Kumazawa, Y.; Maniwa, Y.; Umezu, I.; Suzuki, S.; Ohtsuka, Y.; Achiba, Y. *Synth. Met.* **1999**, *103*, 2555.
(10) Itkis, M. E.; Borondics, F.; Yu, A.; Haddon, R. C. *Nano Lett.* **2007**, *7*, 900.
(11) Yu, A.; Ramesh, P.; Itkis, M. E.; Bekyarova, E.; Haddon, R. C. *J. Phys. Chem. C* **2007**, *111*, 7565.
(12) Hone, J.; Whitney, M.; Piskoti, C.; Zettl, A. *Phys. Rev. B* **1999**, *59*, R2514.
(13) Berber, S.; Kwon, Y. K.; Tomanek, D. *Phys. Rev. Lett.* **2000**, *84*, 4613–6.
(14) Prasher, R. *Phys. Rev. B* **2008**, *77*, 075424–1.
(15) Yang, D. J.; Zhang, Q.; Chen, G.; Yoon, S. F.; Ahn, J.; Wang, S. G.; Zhou, Q.; Wang, Q.; Li, J. Q. *Phys. Rev. B* **2002**, *66*, 165440-1.
(16) Kim, Y. A. K. S.; Tajiri, T.; Hayashi, T.; Song, S. M.; Endo, M.; Terrones, M.; Dresselhaus, M. S. *Appl. Phys. Lett.* **2007**, *90*, 093125/1.
(17) O'Neal, D. P.; Hirsch, L. R.; Halas, N. J.; Payne, J. D.; West, J. L. *Cancer Lett.* **2004**, *209*, 171.

10.1021/cm800428e CCC: $40.75 © 2008 American Chemical Society
Published on Web 05/29/2008

thermal ablation, but their peak absorbance lies within the visible spectrum, thus making gold nanoparticles less than ideal candidates for hyperthermic treatment.[18–22] This shortcoming has been mitigated by the ability to tune the optical properties of the nanoparticles by varying the thickness of a gold layer over a silica core to create gold nanoparticles that are absorbant in the NIR region.[17] Optically tuned gold nanoparticle heating has been successfully quantified in vivo using magnetic resonance temperature imaging, which extrapolates temperature values from the proton resonant frequency shift.[23]

The heating of CNTs by electrical means (ohmic heating) has been directly measured using scanning thermal microscopy.[24] This technique has a very high resolution (lateral resolution of 50 nm) but is subject to the same drawbacks that traditional temperature measurement devices face and might not be well suited to measure laser-induced heating as the probe tip would interfere with the incident light beam that has a diameter of <1 mm. Indirect quantification of CNT heating during laser stimulation has been performed with a traditional temperature probe submersed in a fluid with soluble DNA conjugated single-wall carbon nanotubes.[2] Wavelength-dependent double-walled carbon nanotube heating has also been investigated by measuring the laser power required to heat suspensions in methanol to the vaporization point.[25] Laser-induced CNT heating has been quantified by correlating Raman shift values with known temperature-dependent shifts.[26,27] Interestingly, CNT heating has been shown to be powerful enough to ignite when CNTs are combined with an iron catalyst.[28,29]

Several disadvantages of the current methods using traditional thermocouple and thermistor temperature measurement systems are as follows: (A) trade-offs between fragility and temporal response (smaller, more fragile temperature probes with less mass will more readily change temperature with the environment, providing a faster response time); (B) inconsistencies of thermal properties between the probe tip and the sample being measured which affect the local thermal field and convective and conductive heat losses; (C) the devices and sample will likely have different optical properties, and the probe may absorb the incident laser radiation, introducing error; and (D) temperatures are only measured at a single point, which is not ideal for measuring samples that contain high temperature gradients which result in an averaging effect and may not be suited for determining maximum temperature.[30] Infrared thermography, especially at the microscopic level, can overcome these disadvantages and has been used extensively to quantify temperature during laser ablation to ascertain safety and dosing limits on biological tissue.[31–34] Additional advantages include high temporal (as high as 1000 frames/s, usually 60 frames/s on a progressive scan imager) and spatial resolution (as small as 5 μm, usually 18 μm). Special techniques can be used to increase both the spatial and the temporal resolution.

It is noteworthy that infrared thermography is a valid method of measuring NIR irradiation as the excitation and emission wavelengths are far apart (excitation 1064 nm, measurement band 7.5−13 μm). This separation in wavelength allows for NIR excitation and mid-IR measurement with no overlap.

The present study was performed to experimentally determine the feasibility of using a thermal imaging system to quantify the heating capabilities of milligram-scale preparations of multiwalled carbon nanotubes (MWNTs). The information is important in estimating the necessary dosage of laser light intensity in selective hyperthermia of cancer and other cells and establishing infrared thermography as a valid method to monitor this process. It also quantifies the maximum CNT temperatures attainable due to laser irradiation. Using this method successfully can significantly reduce the time required to test viability of cells as it provides a direct measurement of lethality without requiring time-consuming culturing and staining methods to estimate survival. The use of infrared thermography for temperature measurement has allowed for specific data on laser-mediated heating kinetics of CNTs to be presented here for the first time to our knowledge.

2. Materials and Methods

2.1. Synthesis of MWNTs. MWNTs were prepared by rf chemical vapor deposition on a Fe−Co/$CaCO_3$ (2.5:2.5/95 wt %) catalyst with acetylene as the carbon source. The catalyst was prepared as follows: First, weighted amounts of metal salts $Fe(NO_3)_3 \cdot 9H_2O$ and $Co(CH_3COO)_2 \cdot 4H_2O$ were dissolved into distilled water under agitation. The pH of the solution was adjusted to about 7.0 by dripping ammonia solution in order to prevent release of CO_2 when the carbonates contact the acids. Next, $CaCO_3$ powder support was added to this solution after the metal salts were completely dissolved. Then, the water was evaporated with a steam bath under continuous agitation; the catalyst was further dried

(18) Everts, M.; Saini, V.; Leddon, J. L.; Kok, R. J.; Stoff-Khalili, M.; Preuss, M. A.; Millican, C. L.; Perkins, G.; Brown, J. M.; Bagaria, H.; Nikles, D. E.; Johnson, D. T.; Zharov, V. P.; Curiel, D. T. *Nano Lett.* **2006**, *6*, 587.
(19) Lapotko, D.; Lukianova, E.; Potapnev, M.; Aleinikova, O.; Oraevsky, A. *Cancer Lett.* **2006**, *239*, 36.
(20) Zharov, V. P.; Mercer, K. E.; Galitovskaya, E. N.; Smeltzer, M. S. *Biophys. J.* **2006**, *90*, 619.
(21) Lapotko, D. O.; Lukianova, E.; Oraevsky, A. A. *Lasers Surg. Med.* **2006**, *38*, 631.
(22) El-Sayed, I. H.; Huang, X.; El-Sayed, M. A. *Cancer Lett.* **2006**, *239*, 129.
(23) Hirsch, L. R.; Stafford, R. J.; Bankson, J. A.; Sershen, S. R.; Rivera, B.; Price, R. E.; Hazle, J. D.; Halas, N. J.; West, J. L. *Proc. Natl. Acad. Sci. U.S.A.* **2003**, *100*, 13549.
(24) Cahill, D.; Goodson, K.; Majumdar, A. *J. Heat Transfer* **2002**, *124*, 223.
(25) Bassil, A.; Puech, P.; Tubery, L.; Basca, W. *Appl. Phys. Lett.* **2006**, *88*, 173113–1.
(26) Liu, M.; Jiang, K. L.; Li, Q. Q.; Yang, H. T.; Fan, S. S. *Solid State Phenom.* **2007**, *121*, 123–331.
(27) Li, H. D.; Yue, K. T.; Lian, Z. L.; Zhan, Y.; Zhou, L. X.; S.L., Z.; Shi, Z. J.; Gu, Z. N.; Liu, B. B.; Yang, R. S.; Yang, H. B.; Zou, G. T.; Zhang, Y.; Iijima, S. *Appl. Phys. Lett.* **2000**, *76*, 2053.
(28) Tseng, S. H.; Tai, N. H.; Hsu, W. K.; Chen, L. J.; Wang, J. H.; Chiu, C. C.; Lee, C. Y.; Chou, L. J.; Leou, K. C. *Carbon* **2007**, *45*, 958.
(29) Ajayan, P. M.; Terrones, M.; de la Guardia, A.; Huc, V.; Grobert, N.; Wei, B. Q.; Lezec, H.; Ramanath, G.; Ebbesen, T. W. *Science* **2002**, *296*, 705.
(30) Choi, B.; Pearce, J. A.; Welch, A. J. *Phys. Med. Biol.* **2000**, *45*, 541.
(31) Jansen, E. D.; Le, T. H.; Welch, A. J. *Appl. Opt.* **1993**, *32*, 526.
(32) LeCarpentier, G. L.; Motamedi, M.; McMath, L. P.; Rastegar, S.; Welch, A. J. *IEEE Trans. Biomed. Eng.* **1993**, *40*, 188.
(33) Pfefer, T. J.; Choi, B.; Vargas, G.; McNally, K. M.; Welch, A. J. *J. Biomech. Eng.* **2000**, *122*, 196.
(34) Torres, J. H.; Ghaffari, S.; Welch, A. J. *Med. Biol. Eng. Comput.* **1990**, *28*, 1.

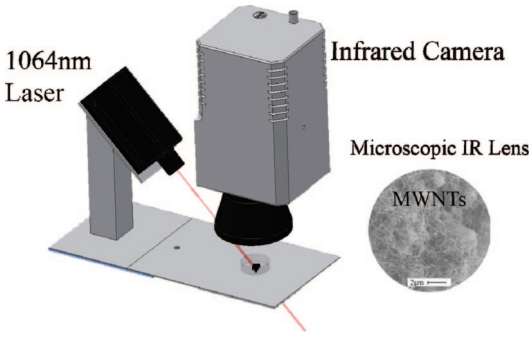

Figure 1. Autodesk Inventor drawing of the experimental setup. Only one laser is shown, but for the 650 nm tests the four lasers were symmetrically placed on all sides of the target area.

Table 1. Sample Numbers and Weights for the 650 and 1064 nm Tests[a]

	650 nm		1064 nm	
sample	MWNT weight (mg)	Graphite weight (mg)	MWNT weight (mg)	Graphite weight (mg)
1	0.6	8.6	2.8	6.7
2	0.5	7.9	3.0	7.8
3	0.05	7.0	2.4	8.0

[a] Sample sizes for the 650 nm tests were chosen to fill the brass well volume, whereas sample sizes for the 1064 nm tests were chosen to ensure that the entire laser spot would strike the sample.

overnight at about 130 °C and further calcined at 500 °C to allow release of the acetates and nitrates from the catalyst. The synthesis was performed at 620 °C.

2.2. Microthermography of MWNTs Treated with 650 nm Lasers. There is no standard methodology for microthermography. Locating a sample and focusing can be difficult because the sample and background will likely be at the same temperature and therefore indistinguishable in the infrared image. Metal objects are helpful for focusing because tiny imperfections often lead to a different temperature than the bulk material. Metal objects, especially polished ones, have a significantly different emissivity than the sample, so locating the sample is easy even if the sample is the same temperature as the metal. In this experimental setup, a small brass metal stage was used to aid in positioning (horizontal plane) and focusing in on the samples (vertical plane). The brass stage was 0.15875 cm thick and had 0.3175 cm diameter holes punched where the samples were loaded. The brass stage was fixed to a thin (0.3175 cm) layer of polycarbonate. The polycarbonate and brass stage were placed on an adjustable platform for precise focusing (Figure 1).

To test the potential of the system at low power, shorter wavelength lasers, four ordinary red laser pointers (model #90725, Cen-Tech, Camarillio, CA) were used as they are readily available and have an emission (650 nm) that is relatively close to the NIR spectrum. The nominal power of the lasers was listed as 5 mW, but measurements with a Newport Power Meter model 1815-C (Newport Corp., Irvine, CA) showed that the actual power was 2.5 mW, resulting in a power density of 0.026 W/cm^2. They are also inexpensive and relatively nonharmful to biological systems at low power. The laser pointers had a tripod for easy positioning and a push button function for continuous activation. The four 650 nm lasers were positioned on a rigid support frame around the sample and aimed at the target prior to loading the MWNT test or graphite control. The average laser spot size of 3.5 mm was verified with photosensitive paper prior to each experiment. Once the lasers were in place, the samples were weighed (Table 1) and loaded onto the stage.

Table 2. Nominal and Measured Power Levels and Densities for the 650 nm Laser Pointers and the 1064 nm Laser

nominal (mW)	measured (mW)	power density (W/cm^2)
650 nm		
5	2.5	0.026
1064 nm		
250	53	1.687
300	130	4.137
350	231	7.352
400	320	10.185
450	390	12.412

Images of the samples were acquired at 1 Hz and recorded to a sequence file using a calibrated FLIR Thermacam SC500 thermal camera (FLIR Systems, Inc., Boston, MA). The camera lens used has a field of view (FOV) of approximately 4 × 6 mm with a maximum resolution of 18 μm per pixel. Images were recorded for 30 s prior to activation of the first laser, and each laser source was activated at 1-min intervals so that at the end of 3 min and 30 s all of the lasers were operating. Images were recorded for an additional minute with all of the lasers activated, the lasers were turned off, and the sample temperature was allowed to equilibrate (assuming there was a temperature increase). For data analysis, FLIR Thermacam Researcher (FLIR Systems, Inc., Boston, MA) sessions were embedded in Microsoft Excel (Microsoft Corp., Redmond, WA) where a Visual Basic Macro was used to extract the maximum temperature values of the target area, which was defined as the entire area inside the diameter of the brass stage. These tests were performed in triplicate, and the averages of maximum-recorded temperatures were plotted versus laser power.

2.3. Infrared Thermography of MWNTs Treated with a 1064 nm Laser. An imaging chamber was constructed so that the external environment was shielded from laser irradiation. The sample and laser (model DP-1064-1000K, Lasermate Group, Inc., Pomona, CA) were positioned and aligned inside this chamber (Figure 1). An opening in the chamber allowed proper positioning of the camera lens for viewing of the sample. The laser was positioned 15.5 cm away from the sample at a 45° angle, and it is coherent at this distance. The beam was not further manipulated and has a Gaussian distribution with a 1/e^2 value of 2 mm. The max power delivered to the sample was determined to be 12.412 W/cm^2 at a laser power of 390 mW using a Newport Power Meter model 1815-C (Newport Corp., Irvine, CA). The measured power levels disagreed with the nominal power levels (Table 2). The measured values were assumed correct and are used in this study. The laser was held in place by a steel bar that was bolted to the focusing platform on which the samples rest. This allowed for easy targeting of the sample by ensuring that the laser would strike the sample at the same position, with the same spot size, in each replicate test.

The samples were weighed and positioned on a polycarbonate platform in the path of the laser. Samples were treated at five different power levels (53, 130, 231, 320, and 390 mW, respectively) for 30 s intervals. Thermal images were acquired and processed as described above except that they were recorded on a FLIR A40 infrared camera without the microscopic lens. The normal temperature range setting for the camera was used (0−250 °C) for testing, but the extended setting for high temperatures (150−500 °C) was used to measure the temperature of the MWNTs exposed to maximum laser power. Graphite (Pentel of America Inc., Torrance, CA) was used in parallel as a control since it is an allotrope of carbon and geometrically presented as unrolled sheets of graphene layers stacked in plane. Moreover, graphite was chosen to illustrate how the specific orientation and rolling of the graphitic sheets as present in the CNTs has an optical absorbance advantage

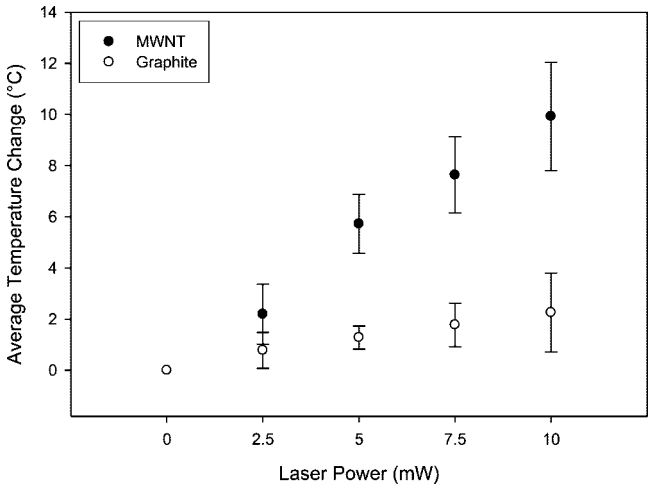

Figure 2. Average maximum temperature increase above baseline of MWNTs and graphite vs power while being treated with four 650-nm/2.5-mW laser sources in succession (mean ± std).

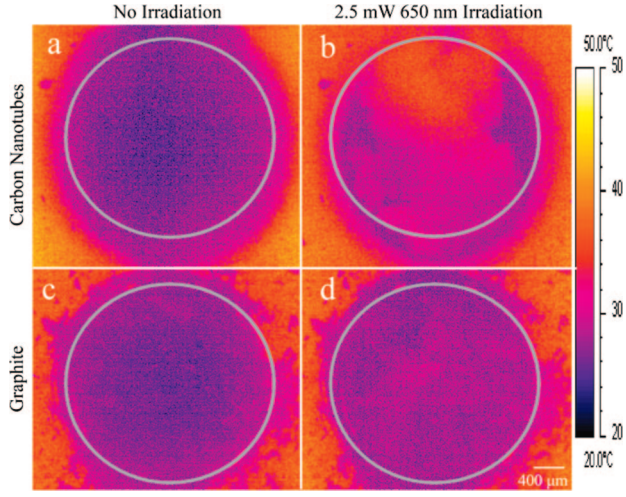

Figure 3. Infrared images before (a and c) and during laser treatment (b and d) with four 650-nm/2.5-mW lasers. Images are of MWNTs (a and b) and graphite (c and d) with the target area inside circle.

over other carbon allotropes, resulting in improved thermal capabilities, with better electron−phonon interaction at the level of CNTs vs graphene.[35] Tests were performed in triplicate with fresh samples. The maximum and average temperature of the treatment area (which was the same for both tests and controls) were extracted and averaged.

3. Results and Discussions

The MWNTs treated with the 650 nm laser irradiation showed a modest 6−7 °C increase over the graphite control and a 10 °C increase over baseline (Figure 2). This small increase is encouraging given the very low power of the lasers (5 mW, indicated; 2.5 mW, measured, each). Examination of infrared images clearly indicates the heating of the MWNTs, while the temperature increases for graphite shows only a slight change (Figure 3). The maximum temperature follows a linear relationship with the power level of the laser used. The heating of the CNTs was typically localized in the top of the image, as this was the direction of the incident

(35) Samsonidze, G. G E. B.; Saito, R.; Jiang, J.; Dresselhaus, G.; Dresselhaus, M. S. *Phys. Rev. B* **2007**, *75*, 155420/1.

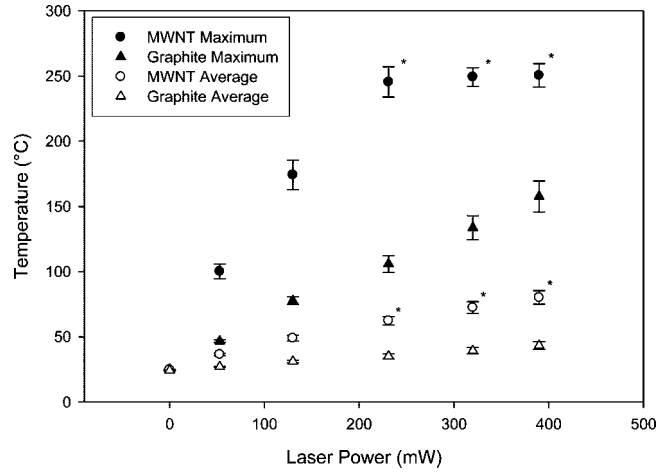

Figure 4. Maximum and average temperatures in the target area of MWNTs and graphite as a function of laser power level. Graphite exhibited much lower temperatures than the MWNTs. The asterisk (*) indicates that the actual temperatures of the MWNTs were above the camera detection limit of 265 °C, causing the maximum temperature to be the same for the 231, 320, and 390 mW power levels, thus resulting in a slight error for the average temperature values.

lasers. This trend was not seen in the graphite samples as they more readily conformed to the stage (they were aligned in parallel and did not protrude over the brass stage) and did not prevent the laser from targeting the entire sample. The small variations in the temperature distribution could also be attributed to imperfect direction and alignment of the four lasers toward the target.

The MWNTs treated with the higher power 1064 nm laser showed a much larger increase in temperature. During the 390 mW treatments, the target areas maximum temperature was at or above the 265 °C limit of the camera's normal recording range (Figure 4). These temperatures are significantly higher compared to the maximum temperature recorded for graphite of 160 °C at 390 mW. The temperature follows a linear increase for the graphite starting with the 53 mW of power. However, for the MWNTs the linearity is more difficult to infer due to saturation of the camera sensor at the high temperatures. From the three measurements within the range of the camera (only one replicate of the 231 mW power level exceeded the detection limit) it seems that the increase is also linear (Figure 4). During similar tests with the camera detection range set to 150−500 °C, the 390 mW treatments reached approximately 305 °C. Such a variation in the temperature measurements can be explained by the random orientation of the MWNTs in the sample (presenting itself as a porous surface to both the laser beam and the infrared camera), affecting the absolute thermal conductivity and the possible variation in the sample thickness, which is known to affect the optical absorption of laser radiation by the MWNTs.[15]

The average target temperatures were also significantly higher for MWNTs than for graphite (Figure 4). In this case, the linearity of average temperatures with the power level is obvious for both MWNTs and the graphite control. Plotting the temperature increase versus time reveals that the MWNTs reached their maximum temperature much faster than the graphite (Figure 5). The increase in average temperature for both MWNTs and graphite was approximated by a first-order equation as a function of time using the least-squares method

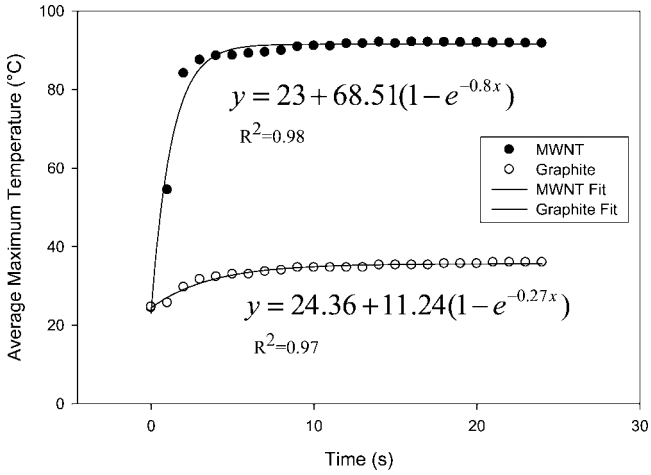

Figure 5. Maximum temperature vs time for the 53 mW treatment of the MWNTs with the 1064 nm laser.

with a coefficient of determination of 98%. Other equations tested for goodness of fit, including hyperbolic, polynomials, and power functions of time, yielded lower coefficients of determination using the least-squares analysis. The time constants for the first-order equation in the case of MWNTs was determined to be approximately 1 s, three times smaller than for the graphite control, illustrating the speed with which the MWNTs heat in the presence of laser light. By comparison, using other methods for temperature measurements, such as dissolving them in water, requires a long time lag for the water to heat prior to measuring its temperature (2 min to reach 75 °C).[2] Other CNT stimulation methods, such as radiofrequency, achieved heating rates of only 7 K/s at 600 W of power compared to the rate of more than 100 K/s in this study at only 53 mW of power.[36] This extremely rapid increase in temperature indicates that the kinetics of laser absorption is ideal for photothermal ablation applications due to its high photon−phonon interaction in the CNTs during laser irradiation compared to other types of electromagnetic energy excitation.

The thermal properties of CNTs, including their specific heat, thermal conductivity, and thermopower, strongly depend on the phonon dispersion relations and the phonon density of states since for 3D crystalline graphite and 2D graphene layers, from which CNTs are derived, the dominant contribution to the heat capacity comes from the phonons, while the electronic contribution is so small that it can be essentially neglected.[37] Each CNT is excited to the electronic excited state, followed by a rapid relaxation to the ground state with an effective electron−phonon conversion of the absorbed photon energy into thermal energy. Because of the very fast heat diffusion time, thermal energy rapidly diffuses along the CNT wall and then to the medium inside and outside of the wall. Because the low-frequency phonons for an isolated CNT have different characteristics from 2D/3D graphite and especially differences in the low-frequency phonon density of states, we expect the specific heat for the CNTs to have a different temperature dependence than that

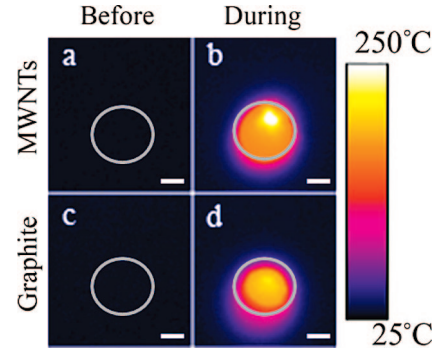

Figure 6. Infrared images before (a and c) and during laser treatment (b and d) at a power intensity of 320 mW for MWNTs (a and b) and graphite (c and d) with the target area inside the circle (scale bars in the lower right corners are 4 mm). MWNT temperatures exceeded the 265 °C limit for the normal range of the infrared camera.

for a 2D/3D graphite. Thus, the laser pulse simultaneously heats most of the MWNT's multiple absorbing carbon layers and most of the individual MWNTs in clusters considering MWNT's specific optical properties with dominant scattering and diffraction phenomena compared to optically nontransparent conventional particles like carbon nanoparticles.

The infrared images of the MWNTs and the graphite reveal the spatial heating patterns (Figure 6). The bright regions in the images represent the hot spots, while the dark regions represent colder temperatures. The highest sustained temperature achieved during the experiments was 330 °C with the 1064 nm laser set at full power (1 W, not presented in graphs), which resulted in the melting of the polycarbonate stage and some of the MWNTs becoming embedded (Figure 7). The maximum temperatures reached during these tests were lower than previously reported in laser heating of CNTs as measured by correlation to Raman shift values of known temperature changes.[26,27] These differences are difficult to interpret due to differences in laser intensity, wavelength, CNT structure, and pressure (one of the studies was performed in a vacuum, where much higher temperatures are observed).

Measurement of the spatial and temporal temperature distribution in MWNTs using infrared thermography stimulated with laser radiation has advantages over other methods as it is extremely fast, does not interfere with the absorption of laser light, and was able to determine maximum and average temperatures of samples in a repeatable, dose-dependent manner in real time. The thermographic approach was also beneficial as it does not interfere with the sample temperature distribution or with conductive and convective heat losses from the sample.

The results presented in this work can be explained by the laser radiation interaction with the electronic and phononic structure of the carbon materials. In the optical absorption process presented in this work, the MWNTs were found to reach much higher temperatures compared to the graphite particles. These measurements can be explained by the unique electronic structure and density of states in CNTs that are different than in graphite as well as due to the much higher reflectance of the graphite.[38,39] The thermal effects in CNTs can be mainly

(36) Gannon, C. J.; Cherukuri, P.; Yakobson, B. I.; Cognet, L.; Kanzius, J. S.; Kittrell, C.; Weisman, R. B.; Pasquali, M.; Schmidt, H. K.; Smalley, R. E.; Curley, S. A. *Cancer* **2007**, *110*, 2654.
(37) Dresselhaus, M. S.; Eklund, P. C. *Adv. Phys.* **2000**, *49*, 705.
(38) Dresselhaus, M. S.; Dresselhaus, G.; Saito, R.; Jorio, A. *Annu. Rev. Phys. Chem.* **2007**, *58*, 719.

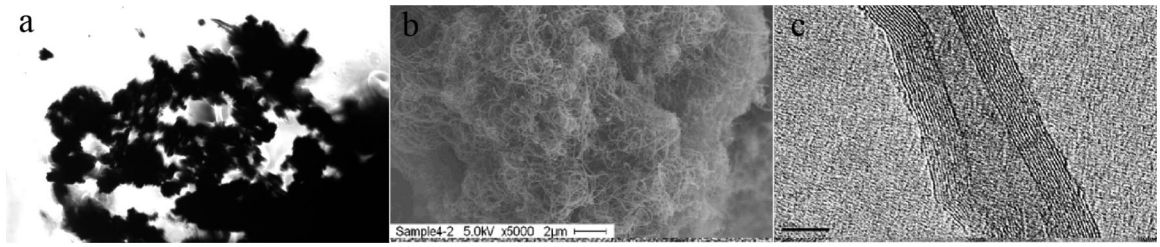

Figure 7. Aggregates of MWNTs that have been heated with a 1 W 1064 nm laser for 4 min shown at 20× magnification (a), and the corresponding high- and low-resolution TEM images of nonirradiated samples (c and b, respectively).

explained by the heat generated during the multiphonon processes involved in the recombination of the electron−hole pairs generated by the laser radiation. In graphite, the thermal conductivity, which is dominated mostly by the phonons, is limited typically by the size of the structural crystallites with the thermal conductivity increasing with the temperature of the sample.[10,14] The presence of large-size crystallites in CNTs could indicate a potential higher 1-D thermal conductivity of the CNTs compared to graphite. Therefore, heating of CNTs exposed to laser irradiation is mostly explained by the heat transfer from the highly excited electrons to the crystalline structure due to the electron−phonon scattering effects and the lower CNT absorbance compared to that of graphite.[36] Given these considerations, the laser heating of CNTs is strongly dependent upon the laser wavelength and laser power per unit of surface.

Because CNTs are extremely hydrophobic, surface functionalization is normally employed to permit dispersion in aqueous media and can also serve as a method for targeting specific cells.[2,40,41] CNTs can be either covalently or noncovalently functionalized with a wide range of substances including polymers, surfactants, nucleic acids, and antibodies.[2,40,41] Studies have been conducted to investigate the toxicology of CNTs in mammalian cells, and the general consensus is that CNTs are not extremely toxic at low levels and that surface functionalization further reduces the level of toxicity.[42,43] Further studies need to be conducted to evaluate the specific cellular uptake of functionalized CNTs in mammalian and human cells as well as the in vitro effect of targeted NIR laser-induced thermal ablation. In this case, there is potential for the functionalized CNTs to nonspecifically bind to unintended targets, increasing the potential for heating of nontarget cells and organs. The MWNTs used in this study were found to reach extremely high temperatures that would be highly detrimental to biological tissues. Studies have shown that temperatures above 40 °C are sufficient for hyperthermia due to protein denaturation and temperatures above 85 °C induce conformational changes in DNA and RNA.[44–46] Such temperatures would be extreme to use, even in a hyperthermia treatment, and would not likely be achieved in cellular experiments where CNT concentrations would be much lower. Tests on cells that have targeted biological tissues containing nanoparticles with lasers (808 nm) have used a similar power density to those used in this test of 3.5−4 W/cm^2.[2,17,23] At the power levels tested in this study, the power densities were 1.687, 4.137, 7.352, 10.185, and 12.412 W/cm^2. From the results presented here, it appears that that the MWNTs studied would be able to provide the necessary increase in NIR absorption to facilitate selective hyperthermia.

4. Conclusion

This study demonstrated for the first time that infrared thermography is an appropriate tool for measuring temperature changes in bulk CNT samples during laser treatment. It was shown that both high- and low-power lasers are sufficient to irradiate CNTs and produce a quantifiable temperature change. The measurement method demonstrated numerous advantages over the traditional measurement techniques and was able to identify and quantify temperature maximums not previously reported. These temperature changes should be biologically significant in the case of targeted hyperthermia of cancer and other cells. CNTs compare favorably to gold nanoparticles in their requirement for low laser power to generate appreciable temperature gains and remain a viable agent for targeted photohyperthermia. While there are reported concerns about the toxicity of CNTs and their use in biological systems, they are not as cytotoxic as some other carbon-based molecules.[47,48] As with most substances that can be detrimental to cell viability, there is likely a tolerable amount of CNTs that will cause little damage. The results demonstrated here suggest that a tolerable dosage of CNTs may be sufficient to act as an efficient agent of photothermal therapy.

Acknowledgment. The authors thank the Department of Biological and Agricultural Engineering and the Louisiana State University Agricultural Center for their financial support of this research project. Published with the approval of the Director of the Louisiana Agricultural Experiment Station as publication # 2008-232-1476.

CM800428E

(39) Yang, Z. P.; Ci, L.; Bur, J. A.; Lin, S. Y.; Ajayan, P. M. *Nano Lett.* **2008**, *8*, 446.
(40) Zheng, M.; Jagota, A.; Semke, E. D.; Diner, B. A.; McLean, R. S.; Lustig, S. R.; Richardson, R. E.; Tassi, N. G. *Nat. Mater.* **2003**, *2*, 338.
(41) Klumpp, C.; Kostarelos, K.; Prato, M.; Bianco, A. *Biochim. Biophys. Acta* **2006**, *1758*, 404.
(42) Lacerda, L.; Bianco, A.; Prato, M.; Kostas, K. *Adv. Drug Deliv. Rev.* **2006**, *58*, 1460.
(43) Smart, S. K.; Cassady, A. I.; Lu, G. Q.; Martin, D. J. *Carbon* **2006**, *44*, 1034.
(44) Huang, X.; Jain, P. K.; El-Sayed, I. H.; El-Sayed, M. A. *Photochem. Photobiol.* **2006**, *82*, 412.
(45) He, X.; Wolkers, W. F.; Crowe, J. H.; Swanlund, D. J.; Bischof, J. C. *Ann. Biomed. Eng.* **2004**, *32*, 1384.
(46) Lepock, J. R. *Int. J. Hyperthermia* **2003**, *19*, 252.
(47) Ding, L.; Stilwell, J.; Zhang, T.; Elboudwarej, O.; Jiang, H.; Selegue, J. P.; Cooke, P. A.; Gray, J. W.; Chen, F. F. *Nano Lett.* **2005**, *5*, 2448.
(48) Magrez, A.; Kasas, S.; Salicio, V.; Pasquier, N.; Seo, J. W.; Celio, M.; Catsicas, S.; Schwaller, B.; Forro, L. *Nano Lett.* **2006**, *6*, 1121.